NASA Technical Paper 1036

Experimental Flow Coefficients of a Full-Coverage Film-Cooled-Vane Chamber

Peter L. Meitner and Steven A. Hippensteele

SEPTEMBER 1977

NASA Technical Paper 1036

Experimental Flow Coefficients of a Full-Coverage Film-Cooled-Vane Chamber

Peter L. Meitner
Lewis Directorate,
U.S. Army Air Mobility R&D Laboratory
and
Steven A. Hippensteele
Lewis Research Center
Cleveland, Ohio

National Aeronautics
and Space Administration

**Scientific and Technical
Information Office**

1977

EXPERIMENTAL FLOW COEFFICIENTS OF A FULL-COVERAGE FILM-COOLED-VANE CHAMBER

by Peter L. Meitner and Steven A. Hippensteele

Lewis Research Center and
U. S. Army Air Mobility R&D Laboratory

SUMMARY

Ambient- and elevated-temperature flow tests were performed on a four-times-actual-size model of an impingement- and film-cooled chamber (full-coverage film cooling) of a core engine turbine vane. Flow tests were conducted in a tunnel with the impingement and film cooling plates combined as a chamber and with the impingement plate removed from the film cooling plate. These tests were conducted at ambient- and elevated-temperature conditions with main-stream gas flow Mach numbers from 0 to 0.95. Coolant supply pressures and temperatures ranged from ambient to 68.5 N/cm^2 and 787 K (99.3 psia and 956° F), respectively. Main-stream gas flow pressures and temperatures ranged from ambient to 50.8 N/cm^2 and 1150 K (73.7 psia and 1610° F), respectively. Further ambient bench tests were conducted with the separated impingement and film cooling plates over pressures ranging from 10.2 to 29.7 N/cm^2 (14.8 to 43.1 psia).

The flow through the impingement holes was treated in terms of a discharge coefficient (CD_i), and the flow through the film cooling holes into still air (no main-stream gas flow) was treated in terms of a total-pressure-loss coefficient (KT_{nmg}). The effects of main-stream gas flow on the flow through film cooling holes were expressed as a function of the coolant to main-stream gas momentum flux ratio.

For measured data used directly, both the impingement discharge coefficient CD_i and the film cooling total-pressure-loss coefficient for flow into still air KT_{nmg} showed appreciable data scatter. A smoothing technique was developed to identify and reduce measurement scatter. Measured data were plotted against an appropriate correlating parameter that reduced the data to a form easily fitted by a polynomial curve. Values of weight flow for the flow coefficient calculations were obtained from the corresponding correlation curves.

For given supply and downstream pressures across each plate, the impingement flow was reduced by the presence of the downstream film cooling plate, but the film cooling flow was not affected by the presence of the upstream impingement plate.

INTRODUCTION

Full-coverage film cooling is a very effective scheme for protecting turbine components from the hostile operating environment of high main-stream gas temperature and pressure. Compressor discharge cooling air is first impinged on the inside of the vane or blade shell to remove heat by convection. The cooling air is then bled out through a large number of evenly distributed holes in the vane or blade outer surface. The coolant forms a continuous, relatively cool, insulating layer between the outer surface and the hot main-stream gas. Full-coverage film cooling (FCFC) permits increased engine operating temperatures and pressures for greater overall cycle efficiency (lower specific fuel consumption) while keeping required coolant flow rates at acceptable levels.

In designing FCFC hardware, it is essential that the flow and distribution of cooling air within a vane or blade be known accurately. This requires the experimental determination of flow coefficients for coolant flow through closely spaced impingement and film cooling plates. Such flow coefficients are expressed either as a discharge coefficient CD or as a total-pressure-loss coefficient KT, the choice of parameter usually being determined by the flow geometry. Both coefficients can be found in the literature (refs. 1 to 6). Reference 1 establishes flow coefficients for multiholed orifice plates in a circular conduit, and references 2 and 3 establish flow coefficients for varied cooling configurations such as leading-edge impingement, impingement with crossflow, flow through film cooling holes, and trailing-edge ejection. Reference 4 examines the effect of approach flow inclined to the orifice axis, and reference 5 establishes flow coefficients for film cooling holes discharging into main-stream gas flow at several Mach numbers. Reference 6 presents data that attempt to isolate the effects of main-stream gas flow on the flow through film cooling holes.

Despite numerous flow coefficient experiments, no investigators have combined impingement and film cooling geometries in a manner resembling full-coverage film cooling. Furthermore, few investigations have been performed that clearly isolate the effects of main-stream gas flow on the flow through film cooling holes. The experimental flow tests described herein were designed to provide this information for a particular geometry. Tests were performed on a four-times-actual-size model of a typical FCFC vane geometry to determine flow coefffficients for impingement and film cooling holes. Furthermore, the effects of main-stream gas flow on the flow through film cooling holes were established for a broad range of coolant flow and main-stream gas Mach numbers. Tests were conducted in a tunnel with main-stream gas Mach numbers between 0 and 0.95 at coolant temperatures from ambient to 787 K (956° F). The impingement and film cooling plates were also tested separately in ambient bench tests. Coolant flow Reynolds numbers for the impingement and film cooling plates ranged from 5000 to 90 000 and 2000 to 38 000, respectively. These values bracket the range of Reynolds numbers for an actual-size, high-temperature vane or blade design, which vary from 19 000 to 78 000

for the impingement holes and from 13 000 to 32 000 for the film cooling holes.

Flow coefficients can be expressed as a function of either Reynolds number or Mach number. Reference 7 discusses the applicability of each parameter for given flow situations. While no general rule is established, it is pointed out that, for discharge coefficients, the Reynolds number may be the suitable correlating parameter at low velocities but the Mach number may be necessary for high-velocity flows. The test data were analyzed in terms of both Reynolds number and Mach number. Both parameters gave approximately the same amount of data scatter, but using Mach number allowed a smoothing technique to be used that identifies and helps reduce flow measurement data scatter. The flow characteristics through the impingement and film cooling holes (for no main-stream gas flow) were therefore described as functions of Mach number in terms of a discharge coefficient and a total-pressure-loss coefficient, respectively. The effects of main-stream gas flow on the flow through film cooling holes were expressed in terms of the coolant to main-stream gas momentum flux ratio.

APPARATUS

Flow tests were conducted in a flat-plate heat transfer tunnel with a film cooling plate alone and with a film cooling plate and an impingement plate combined to form a chamber. In addition, bench tests were conducted with the individual impingement and film cooling plates. The tunnel is illustrated in figure 1. The test section is 9.86 centimeters (3.88 in.) wide and 8.89 centimeters (3.50 in.) high. Vitiated main-stream gas flow can be supplied at pressures to 100 N/cm^2 (150 psia) and temperatures to 1200 K (1700^o F); unvitiated cooling air is available to 100 N/cm^2 (150 psia) and 810 K (1000^o F).

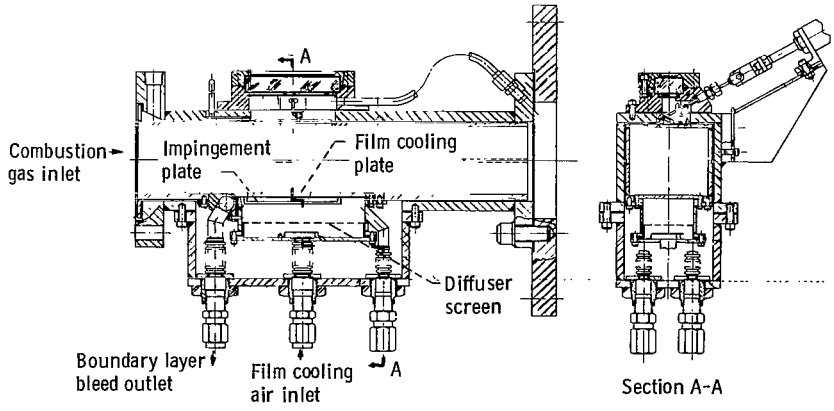

Figure 1. - Combined impingement and film cooling plates (chamber) installed in heat transfer tunnel.

The test-plate, initial boundary-layer thickness is controlled by a bleed slot immediately upstream of the test plate.

The test plates are shown in the combined configuration in figure 2. The impingement and film cooling plates have 6 and 12 rows of holes, respectively. The impingement plate is 0.16 centimeter (0.065 in.) thick and the film cooling plate is 0.47 centimeter (0.185 in.) thick, with an impingement distance of 0.61 centimeter (0.24 in.) between the plates. Hole spacings and hole sizes are shown in figure 2, along with the inclination angles of the film cooling holes. Note that these angles vary from row to row.

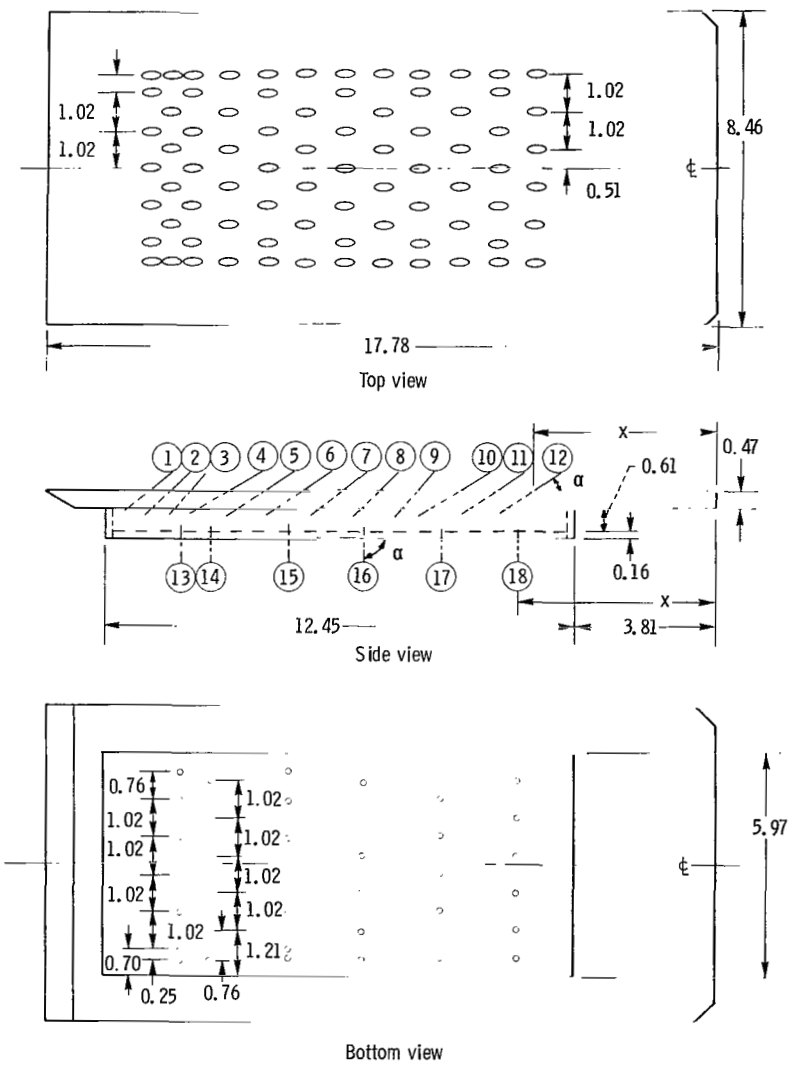

Row	Number of holes	Angle, α deg	Diameter, cm	Distance from trailing edge, x, cm
1	7	39	0.132	14.99
2	6	45	.132	14.48
3	7	50	.132	13.97
4	6	31	.142	12.95
5	7	34	.142	11.94
6	6	35	.142	10.92
7	7	39	.132	9.91
8	6	45	.132	8.89
9	7	50	.132	7.87
10	6	31	.142	6.86
11	7	34	.142	5.84
12	6	35	.142	4.83
13	7	90	.132	14.22
14	6	↓	↓	13.46
15	7	↓	↓	11.43
16	6	↓	↓	9.40
17	7	↓	↓	7.37
18	6	↓	↓	5.33

Figure 2. - Combined impingement and film cooling plate configuration. (All dimensions in cm.)

In the modeled vane chamber the hole angles are constant with respect to the chord line. However, because of the curvature of the vane outer surface, the coolant-hole exit angles with respect to the outer surface vary from row to row. All angles are in line with the main-stream gas flow. Several views of the test plates are shown in figure 3.

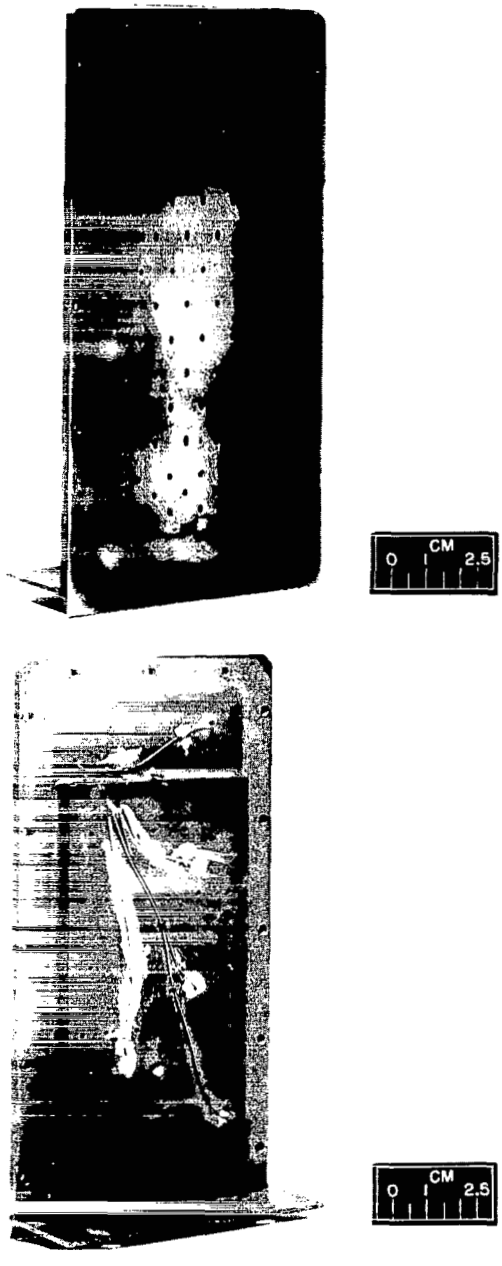

Figure 3. - Combined impingement and film cooling plates.

INSTRUMENTATION

The instrumentation for the tunnel tests is shown in figure 4. Supply and plenum pressure were each measured at three locations. One of the plenum pressure measurements was taken as the reference pressure (indicated in fig. 4). This pressure was measured on a 0- to 69-N/cm^2 (0- to 100-psig) gage, and all other pressures were obtained by measuring differences from the reference pressure with gages calibrated in inches of water. Two static pressure taps were located on the film cooling plate as shown. Main-stream gas total temperature and pressure were measured upstream of the film cooling plate. The main-stream gas Mach number over the test plate was determined from the rearmost plate static pressure tap and from a total pressure probe just downstream of the plate. The desired main-stream gas Mach number was set (with no cooling airflow) by regulating the supply pressure and a downstream throttling valve. Coolant flow measurements were made with either a 0.5- or 1.0-centimeter- (0.2- or 0.4-in.-) diameter venturi for low and high flow rates, respectively.

Instrumentation for the separated impingement and film cooling bench tests is shown in figure 5. Each plate was mounted in a fixture identical to that used in the combined tunnel tests. Flow rate was measured by an appropriately sized rotameter. Because of the simplicity of the test setup and the directness of the test measurements, the bench test results are considered the most accurate of all the test results.

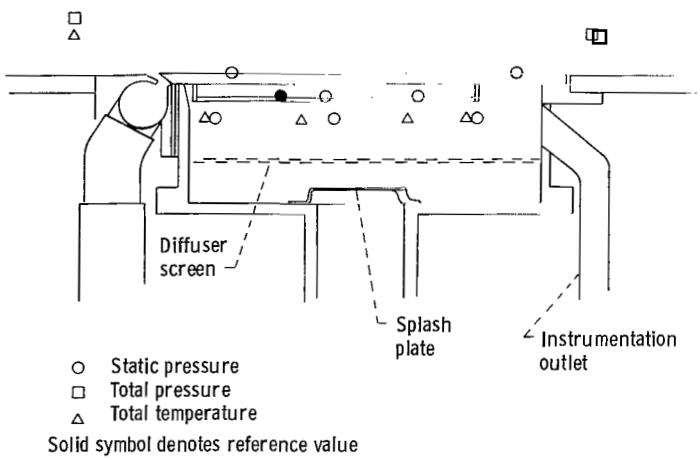

Figure 4. - Tunnel test instrumentation.

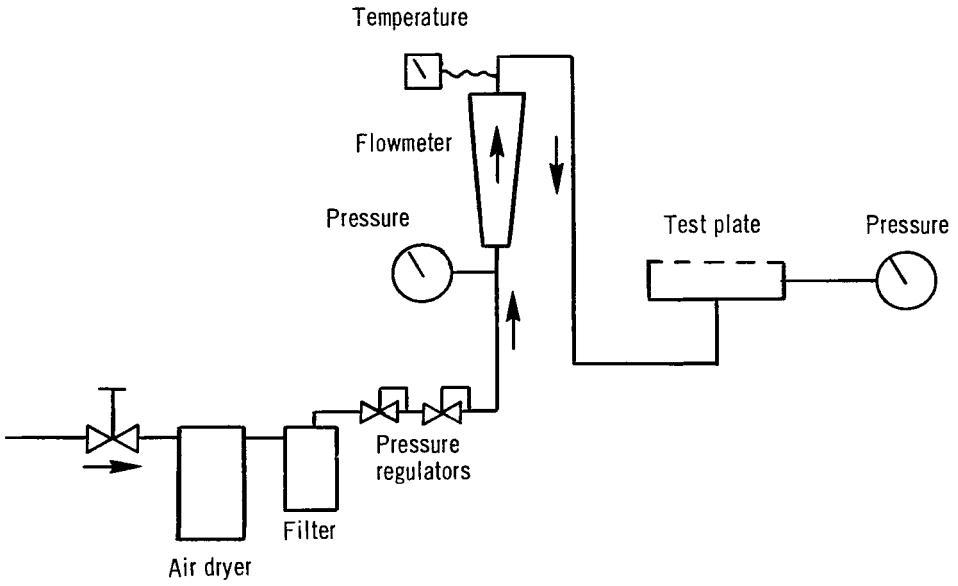

Figure 5. - Bench test instrumentation.

TEST PROCEDURE

The test results are summarized, in 15 groups, in table I. Each group represents a number of runs in which only the coolant supply pressure was varied (except group 13, in which the coolant temperature was also varied). Eight groups of tunnel tests were performed with the combined configuration (impingement and film cooling plates back to back, forming a chamber); five groups were conducted with only the separated film cooling plate. Of the 13 groups of tests performed in the flat-plate tunnel, 10 were at ambient coolant temperature and three at elevated coolant temperature. The two bench tests were performed with the separated impingement and film cooling plates and only at ambient temperature. Tables II to IV list the pertinent test data for all test runs.

ANALYSIS

Figure 6 shows a typical full-coverage-film-cooled chamber discharging into the main-stream gas flow. Station 1 defines the supply conditions, station 2 the impingement orifice plane, station 3 the impingement plenum, and stations 4 and 5 the inlet and outlet of the film cooling holes, respectively. Station 6 defines the static pressure of the main-stream gas flow. It is assumed that the total pressures at stations 1 and 3 are equal to their respective static pressures because of the comparatively low velocities in

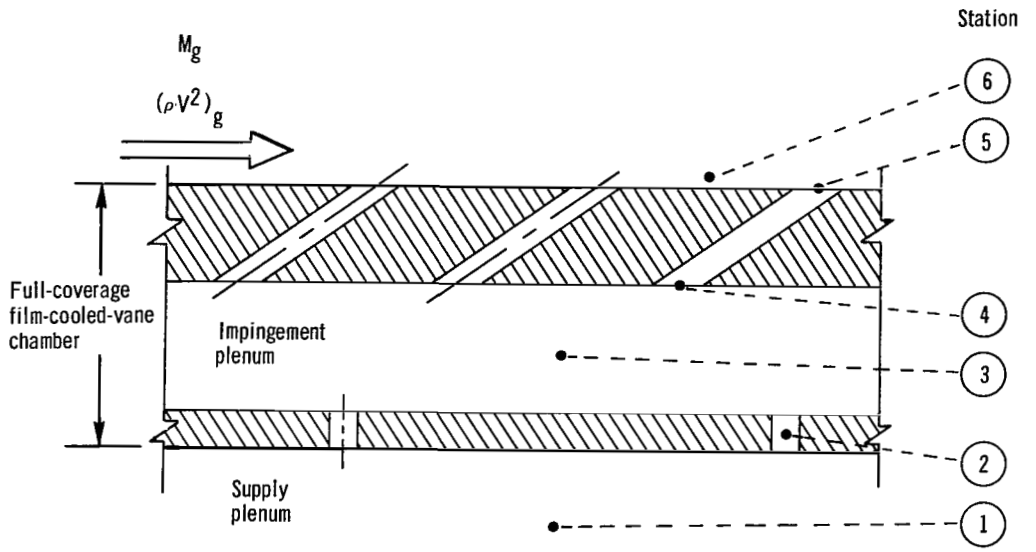

Figure 6. - Full-coverage, film-cooled-chamber station identification.

the supply and impingement plenums. Also, the total temperature is assumed to be constant throughout (no heat transfer taking place).

During the tests, coolant supply and plenum pressures were each measured at three locations and gave almost identical readings. The pressures at these locations were taken to be the average of the three measured pressures. The two static pressure taps on the film cooling plate likewise showed almost identical readings, even for high coolant flow rates. The main-stream gas static pressure at all film cooling holes was thus taken to be the average of the two measured pressures.

Impingement Flow

It is customary (e.g., refs. 2 and 3) to define an impingement orifice discharge coefficient as the ratio of actual to ideal flow by

$$CD = \frac{W_m}{\rho_{2,id} V_{2,id} A_2} \tag{1}$$

where

$$\rho_{2,id} = \frac{p_2}{RT_1'}\left(\frac{p_1'}{p_2}\right)^{(\gamma-1)/\gamma} \tag{2}$$

and

$$V_{2,id} = \sqrt{\frac{2\gamma Rg_c T_1'}{\gamma - 1}\left[1 - \left(\frac{p_2}{p_1'}\right)^{(\gamma-1)/\gamma}\right]} \tag{3}$$

The symbols are defined in appendix A. These formulas require that the impingement jet static pressure p_2 be determined. Since no pressure measurements were made at the orifice plane, an assumption had to be made based on the measured pressures upstream and downstream of the orifice (p_1' and p_3', respectively). It was assumed that for subsonic flow the static and total pressures at station 2 were equal to the measured pressures p_3' and p_1', respectively. For choked flow, p_2 was determined from the assumed inlet total pressure p_1' and the compressible flow relations at Mach 1.0.

Film Cooling Flow into Still Air

A total-pressure-loss coefficient is often used instead of a discharge coefficient (ref. 2) to describe the flow through film cooling holes. The incompressible form of the total-pressure-loss coefficient is usually written as

$$KT = \frac{\Delta(p')}{\frac{1}{2g_c}\rho_j V_j^2} \tag{4}$$

where the change in total pressure is taken from the supply station to a station downstream of a hole. Such a definition, however, couples the flow through the hole with the effects of main-stream gas flow. To isolate the effects of main-stream gas flow and to reflect compressible flow relations, the film cooling hole total-pressure-loss coefficient for flow into still air was defined as

$$KT_{nmg} = \frac{p_3' - p_5'}{p_5' - p_5} \tag{5}$$

where p_5 is the static pressure in the film cooling hole at station 5 (equal to measured p_6 for subsonic coolant flow) and p_5' is the total pressure at station 5, which was deter-

mined analytically in an iterative manner as the value that satisfied the measured weight flow. For choked flow, p_5 was again determined from the assumed total pressure p_5' and the compressible flow relations.

Film Cooling Flow into Main-Stream Gas Flow

Once the total-pressure-loss coefficient for no main-stream gas flow was established, the effects of main-stream gas flow could be determined. For all tests with main-stream gas flow, the KT_{nmg} correlation was used to determine what the coolant flow would have been for flow discharging into still air at the same supply and back pressures. The effects of main-stream gas flow were then expressed as the measured coolant flow (with main-stream gas flow) divided by the flow determined from the KT_{nmg} correlation (without main-stream gas flow) as a function of the coolant to main-stream gas momentum flux ratio.

DATA SMOOTHING AND RESULTS

Experimentally determined flow coefficients are quite sensitive to measurement errors, as can be seen by the data scatter in references 2 to 5. The customary procedure has been to calculate CD or KT based on measured values and then try to fit a "best curve" through the results. This procedure is generally unsatisfactory, since the scatter in CD and KT is often so severe that no obvious best curve exists. This is illustrated in figures 7 to 10, which show the impingement flow discharge coefficient and film cooling flow total-pressure-loss coefficient for flow into still air obtained in this manner, plotted against both Mach number and Reynolds number. The data scatter in figures 7 and 8 is typical of that found for discharge coefficients in references 2 to 5. Figures 9 and 10 show greater data scatter than that found for the total-pressure-loss coefficient in reference 2. However, reference 2 uses a different definition of KT, and a direct comparison can thus not be made.

In comparing figures 7 to 10, no obvious advantage can be deduced in plotting the results against Mach number or Reynolds number. Reynolds number plots show that, for all tests, choked flow occurs over a wide range of Reynolds number (solid symbols in figs. 8 and 10). A curve of CD or KT against Reynolds number never brings out physical flow similarity. However, when the results are plotted against Mach number, physical flow similitude occurs for all tests at a common point, this being choked flow at Mach 1.0.

The experimental data of this investigation were thus correlated in terms of Mach number. Furthermore, to overcome the scatter problem, the data were treated in such a way that scatter was identified and smoothed before the data were incorporated into the CD and KT calculations. The details are given in the following subsections.

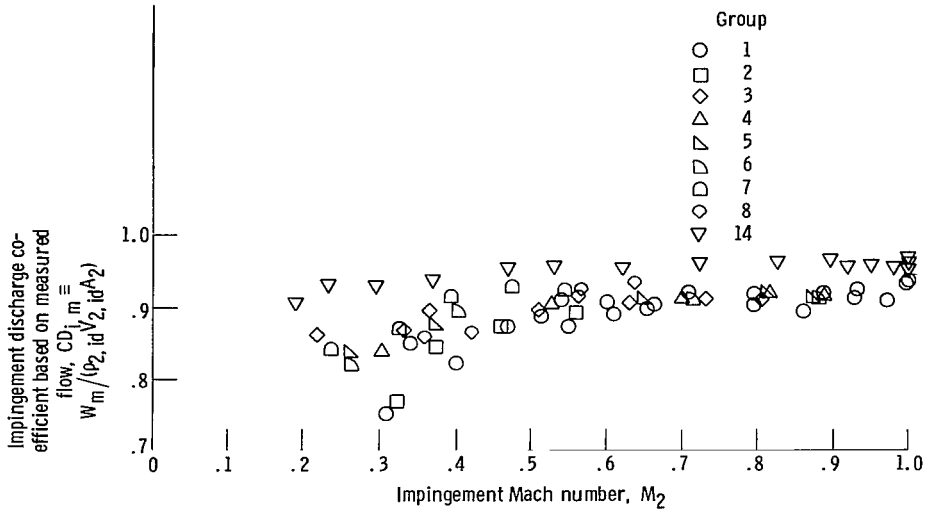

Figure 7. - Impingement discharge coefficient based on measured flow as function of impingement Mach number.

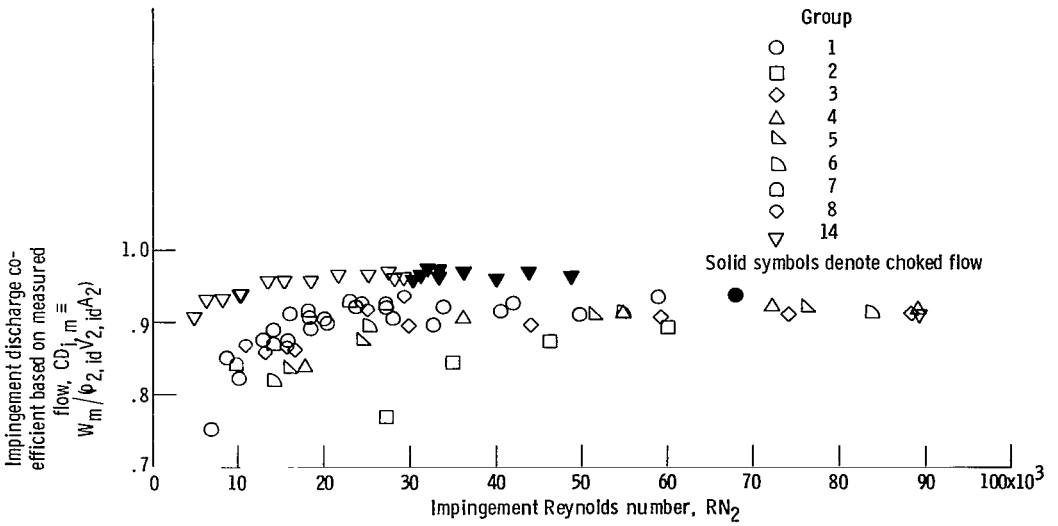

Figure 8. - Impingement discharge coefficient based on measured flow as function of impingement Reynolds number.

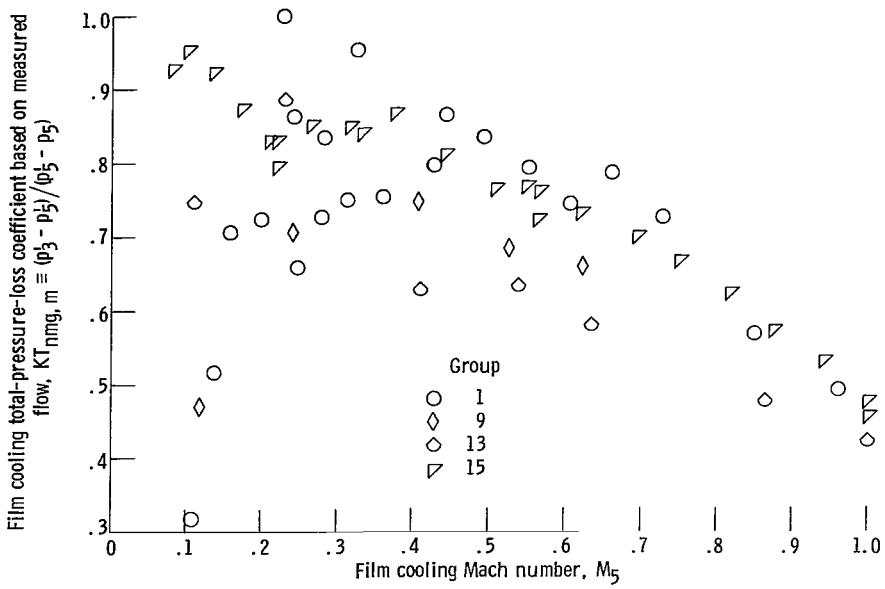

Figure 9. - Film cooling total-pressure-loss coefficient based on measured flow as function of film cooling Mach number.

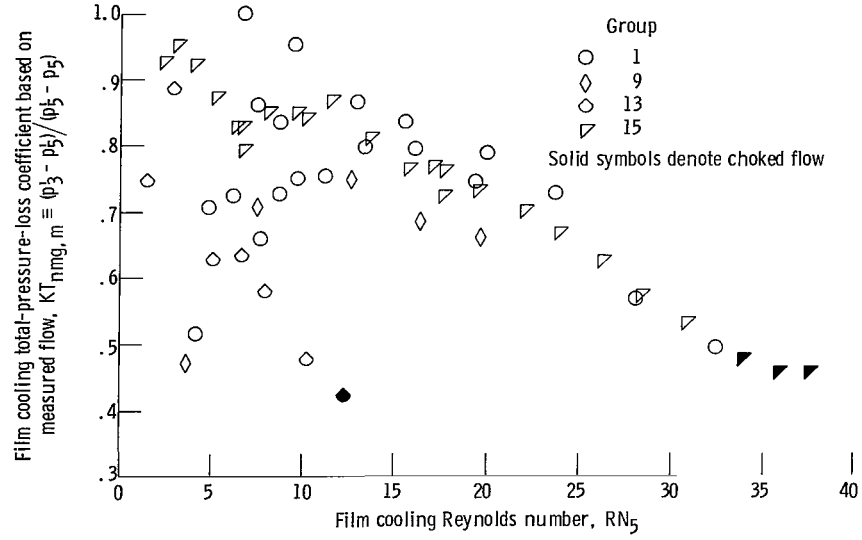

Figure 10. - Film cooling total-pressure-loss coefficient based on measured flow as function of film cooling Reynolds number.

Impingement Flow

Figure 11 shows the nondimensional impingement weight flow function defined by

$$W_{nd,i} = \frac{W_m \sqrt{RT'_1}}{\sqrt{g_c}\, p'_1 A_2} \tag{6}$$

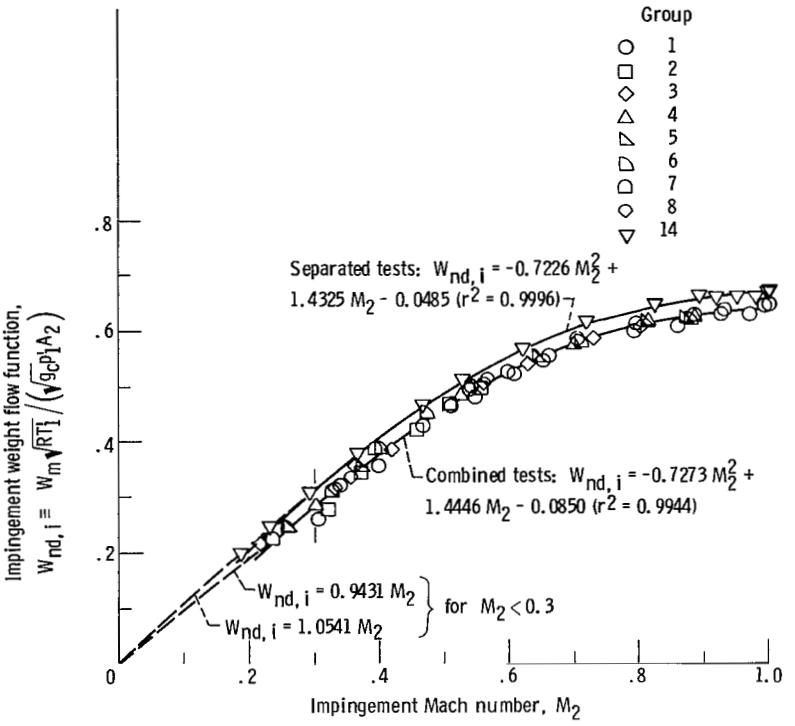

Figure 11. - Impingement weight flow function as function of impingement Mach number (correlated impingement data).

plotted against coolant Mach number. The data of figure 11 fall along two distinct lines. The results of the separated tests form a very well-defined upper line; while the results of the combined tests cluster around a line below the separated test results. The second-order curve-fits through the separated and combined data are shown, along with the goodness of fit (equal to 0.9996 and 0.9944 for the separated and combined tests, respectively). The goodness of fit is defined by

$$r^2 = 1.0 - \frac{\sum_i (y_i - y_{equ})^2}{\sum_i (y_i - \overline{y})^2} \tag{7}$$

The data deviation from the curves of figure 11 can be thought of as the amount of data scatter in the basic test measurements. In particular, if the measured pressures are assumed to be correct (correct M_2), the deviations from the curves of figure 11 can be interpreted as errors in flow measurement; and a new, corrected, weight flow can be calculated from the curves of figure 11 for each data point. Using such "smoothed" values of weight flow instead of $\dot{W}_m$ in equation (1) results in two separate curves of CD_i against M_2, as shown in figure 12. The flow chart for this procedure is shown in appendix B (fig. 16).

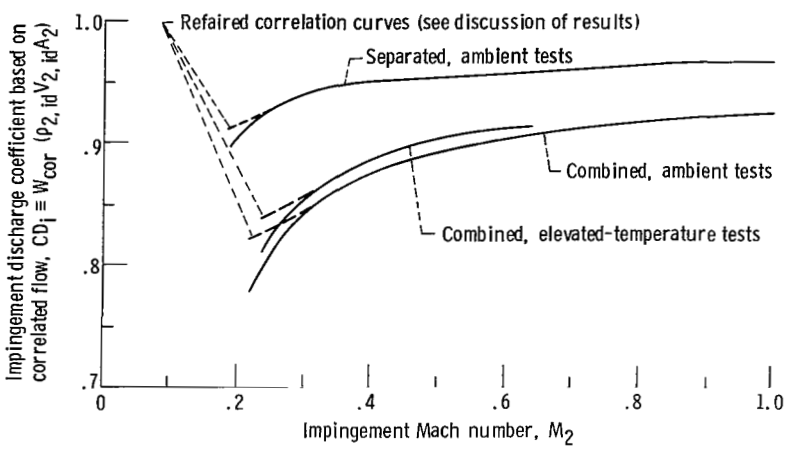

Figure 12. - Impingement discharge coefficient based on correlated flow (from fig. 11) as function of impingement Mach number.

Film Cooling Flow into Still Air

The chosen definition of KT_{nmg} relates p_3', p_5', and p_5. However, p_5' is not measured, and an iteration is required to obtain the value of p_5' that makes the calculated value of weight flow equal to the measured weight flow. As such, a plot of the nondimensional, film cooling, weight flow function against coolant Mach number will result in a continuous curve. Data scatter can be identified, however, if the film cooling, weight flow function

$$W_{nd,fc} = \frac{W_m \sqrt{RT_3'}}{\sqrt{g_c}\, p_3' A_5} \tag{8}$$

is plotted against the parameter Z_{fc}, where

$$Z_{fc} = \sqrt{\frac{\rho_5(p_3' - p_5)}{\rho^*(p_3' - p^*)}} \tag{9}$$

and ρ^* and p^* are the density and pressure at choking as determined from the total conditions p_3' and T_3'. Note that Z_{fc} equals 1.0 at choking. Figure 13 shows $W_{nd,fc}$ plotted against Z_{fc}, along with the "best curve" through the data. Again, if the measured pressures are assumed to be correct, the deviation from the line can be thought of as an error in flow measurement, and a new flow rate can be obtained that will make the data fall on the line in figure 13. The resulting curve of KT_{nmg} against M_5 is shown in figure 14. The flow chart for this procedure is shown in appendix B (fig. 17).

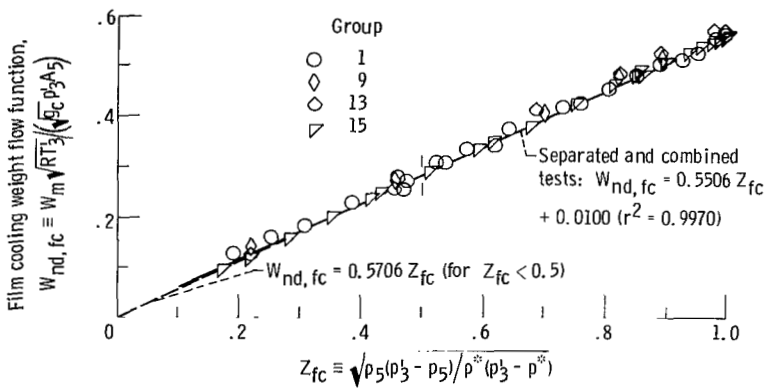

Figure 13. - Film cooling weight flow function as function of parameter Z_{fc} (correlated film cooling data).

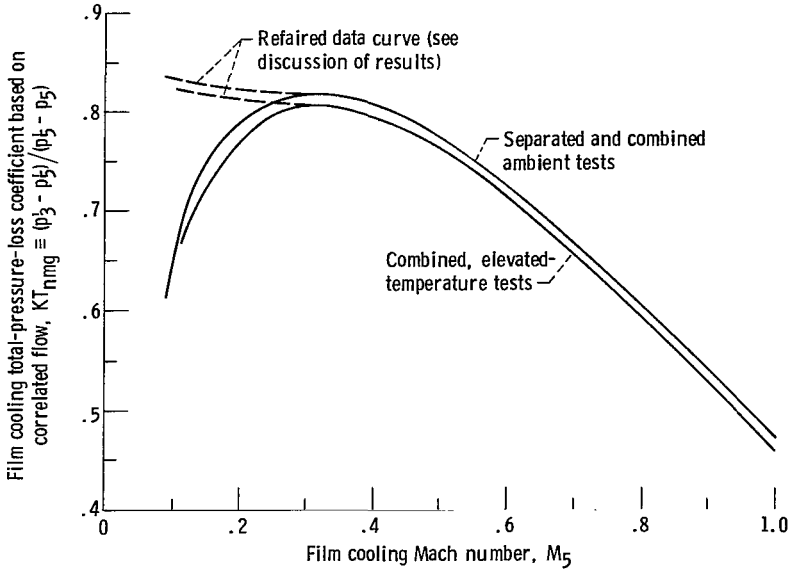

Figure 14. - Film cooling total-pressure-loss coefficient based on correlated flow (from fig. 13) as function of film cooling Mach number.

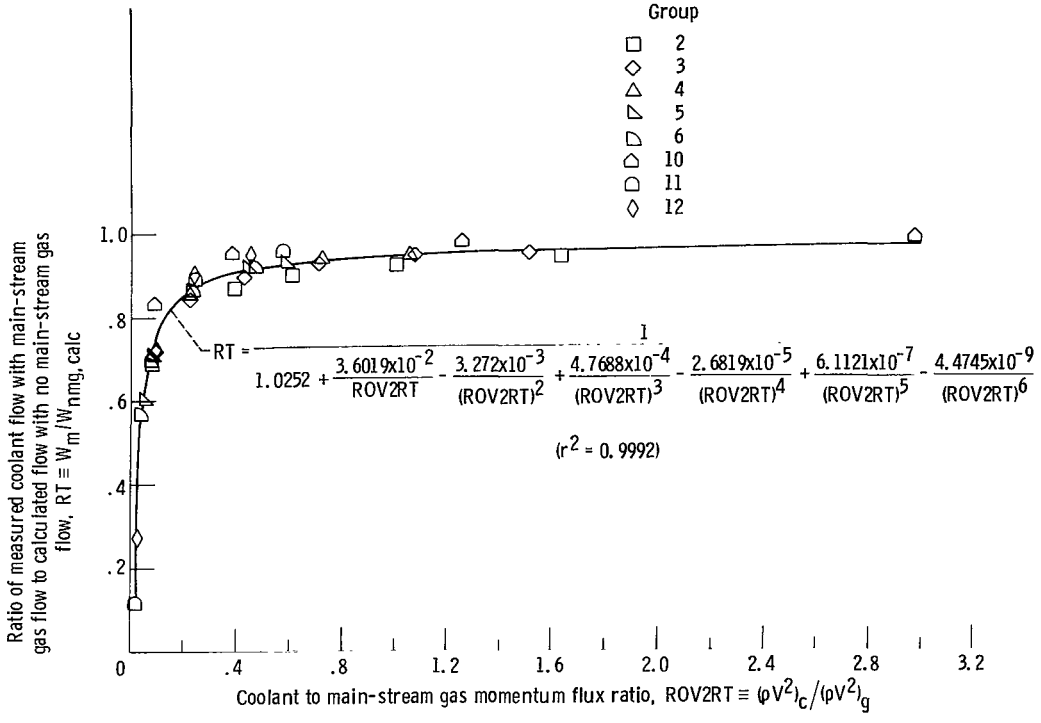

Figure 15. - Effect of main-stream gas flow on coolant flow through film cooling holes.

Film Cooling Flow into Main-Stream Gas Flow

No parameter was found that could be used to smooth film cooling data for test cases with main-stream gas flow. Figure 15 shows the ratio RT of measured coolant flow with main-stream gas flow to calculated coolant flow with no main-stream gas flow $W_m/W_{nmg,\ calc}$ plotted against the coolant to main-stream gas momentum flux ratio $(\rho V^2)_c/(\rho V^2)_g$. Although data scatter is present, the results follow a fairly well-defined curve. The flow chart for the calculation procedure is presented in appendix B (fig. 18). Note that the calculated flow (for no main-stream gas flow) was based on a refaired curve of KT_{nmg} against M_5. The refairing is explained in the next section.

DISCUSSION OF RESULTS

Figures 7 to 10 show the curves of CD_i and KT_{nmg} obtained by using measured values directly. The figures show that CD_i and KT_{nmg} are sensitive to small variations in measured values, especially at low Mach numbers. The sensitivity at the low Mach numbers is compounded by the fact that the greatest measurement errors occur at low flow rates. The curves of figures 11 and 13 ($W_{nd,i}$ against M_2 and $W_{nd,fc}$ against Z_{fc}, respectively) are an attempt to identify and reduce the data scatter by drawing a "best curve" through correlated data before they are incorporated into the sensitive CD_i and KT_{nmg} calculations. As such, the shapes of the "best curves" in figures 11 and 13 are critical to the final CD_i and KT_{nmg} results for low Mach numbers. From an intuitive viewpoint, it is expected that the data in figures 11 and 13 should pass through the origin, since at Mach 0 the flow must equal zero. However, the curve fits in figures 11 and 13 do not pass through the origin, and the shapes of the final CD_i and KT_{nmg} curves at low Mach numbers are therefore suspect. The dashed lines in figure 11 are straight-line refairings that blend into the curve fits at Mach 0.3. Note that for the separated tests, this refairing more closely follows the bench test results, which are considered the most accurate of all the flow measurements. Using the refaired curves results in CD_i curves that differ slightly from the original curves at the low Mach numbers. The new curves are shown as dashed lines in figure 12.

When the curve of $W_{nd,fc}$ against Z_{fc} (fig. 13) was also refaired by a straight line from Z_{fc} of 0 to 0.5 (corresponding to $M_5 \approx 0.3$), the shape of the final KT_{nmg} curve was altered significantly at low Mach numbers (dashed line in fig. 14). Again, note that the refaired curve of figure 13 more closely follows the results of the accurate bench tests. It is therefore believed that the results obtained from the refaired correlation curves more accurately reflect the true curves of CD_i and KT_{nmg}. The results of these calculations show that, while the described method of data smoothing is very useful, great care must still be exercised in treating the data at low Mach numbers because

of the sensitivity of the flow coefficients to variations in mass flow in that flow regime.

In the data-smoothing procedures the impingement flow function $W_{nd,i}$ was plotted against Mach number, and the film cooling flow function $W_{nd,fc}$ was plotted against the parameter Z. The impingement data could also have been smoothed by the parameter Z, but the use of Mach number resulted in a curve that was easier to fit with a polynomial.

The final impingement discharge coefficient and film cooling total-pressure-loss coefficient curves obtained by data smoothing (figs. 12 and 14) show the elevated-temperature results to be slightly different from the ambient results. This difference apparently comes from the fact that, in the elevated-temperature results, thermal expansion of the plates was not accounted for. As the hot coolant flowed through the plates, the hole diameters were expected to increase slightly. When the CD_i and KT_{nmg} calculations were repeated for slightly larger holes, both elevated-temperature results tended toward the ambient curves. The increase in the hole diameter cannot, however, be predicted accurately, since in the short duration of the flow tests, the plates do not reach a uniform temperature. If the increase in hole diameter is calculated on the basis of the maximum temperature difference (hot coolant gas minus ambient conditions), the CD_i and KT_{nmg} results will overcorrect and fall on the other side of the ambient curves of figures 12 and 14.

The calculated impingement discharge coefficients for the combined tests lie between 0.8 and 0.9; for the separated tests they are greater than 0.9 (fig. 12). Most reported discharge coefficients (refs. 2 to 4) lie below 0.9. As such, the calculated values for the separated tests might be questioned. However, there is a difference in geometry between the tests of reference 2 to 4 and this investigation (larger length-diameter ratios in refs. 2 to 4). The geometry of reference 1 comes closest to simulating the geometry of the reported separated tests. Discharge coefficients greater than 0.9 are shown in reference 1, thus giving credence to the reported test results.

Figure 11 and 13 show that, for given supply and downstream pressures, the presence of the downstream film cooling plate reduces the impingement flow and that the presence of the upstream impingement plate has no effect on the flow through the film cooling holes.

SUMMARY OF RESULTS

Ambient- and elevated-temperature flow tests were performed on a four-times-actual-size model of a full-coverage film-cooled segment of a core engine turbine vane. Tests were conducted to establish the flow characteristics through the impingement and film cooling plates combined to form a chamber and with the individual plates separated from each other. The results of the tests are as follows:

1. A method was determined to identify and smooth data scatter. The nondimensional weight flow function was plotted against Mach number or the parameter Z, and smoothed values of weight flow were obtained from the generated correlation curve.

2. The impingement hole discharge coefficients and film cooling hole total-pressure-loss coefficients (for discharge into still air) based on smoothed weight flow correlated very well with coolant hole Mach number.

3. The effects of main-stream gas flow on coolant flow rate through the film cooling holes were correlated by the coolant to main-stream gas momentum flux ratio.

4. For fixed upstream and downstream pressures across each plate, the impingement flow was reduced by the presence of the downstream film cooling plate; the film cooling flow was not affected by the upstream impingement plate.

Lewis Research Center,
National Aeronautics and Space Administration,
and
U. S. Army Air Mobility R&D Laboratory,
Cleveland, Ohio, May 16, 1977,
505-04.

APPENDIX A

SYMBOLS

A	hole area, m^2; ft^2
CD	discharge coefficient
D	diameter, m; ft
g_c	force-mass conversion constant, 1; 32.174 (lbf)(ft)/(lbm)(sec^2)
KT	total-pressure-loss coefficient
M	Mach number
p	pressure, N/m^2; lbf/ft^2
RT	ratio of flows, W_m/W_{nmg}, calc
R	gas constant, J/(kg)(K); ft-lbf/(lbm)(^oR)
RN	Reynolds number, $\rho VD/\mu$ (dimensionless)
r^2	goodness of fit (defined by eq. (7))
T	temperature, K; ^oF
V	velocity, m/sec; ft/sec
W	weight flow, kg/sec; lbm/sec
Z	parameter used in data smoothing
α	angle, deg
γ	ratio of specific heats, C_p/C_v
ρ	density, kg/m^3; lbm/ft^3
μ	viscosity, kg/(m)(sec); lbm/(ft)(sec)

Subscripts:

c	coolant
calc	calculated
cor	correlated
equ	equation
fc	film cooling
g	main-stream gas

i	impingement
id	ideal
j	jet
m	measured
mg	main-stream gas flow
nd	nondimensional
nmg	no main-stream gas flow
1	station at flow inlet (fig. 6)
2	station at impingement orifice
3	station at impingement plenum
4	station at film-cooling-hole entrance
5	station at film-cooling-hole exit
6	station at main-stream gas flow

Superscripts:

'	total conditions
*	choked conditions
‾	average

APPENDIX B

COMPUTER FLOW CHARTS

Computer flow charts for the determination of the impingement discharge coefficient CD_i, the film cooling total-pressure-loss coefficient for no main-stream gas flow KT_{nmg}, and the reduction of film cooling flow due to main-stream gas flow RT are shown in figures 16, 17, and 18, respectively. All calculations properly account for choked flow in the impingement or film cooling holes. The required data input is shown, along with the necessary assumptions.

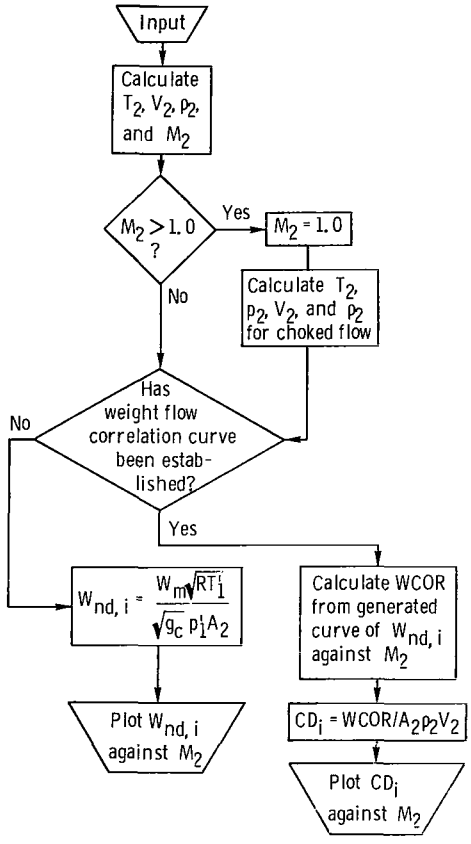

Input:

W_m	measured weight flow
p_1'	supply total pressure
T_1'	supply total temperature
p_3'	plenum total pressure
A_2	area of impingement holes
R	gas constant
$\gamma(T)$	ratio of specific heats as function of temperature
$W_{nd,i}(M_2)$	$W_{nd,i}$ as function of M_2 (established in first pass through calculations)

Assumptions:

$p_2' = p_1'$
$p_2 = p_3'$
$T_2' = T_1'$

Figure 16. - Flow chart for impingement discharge coefficient determination.

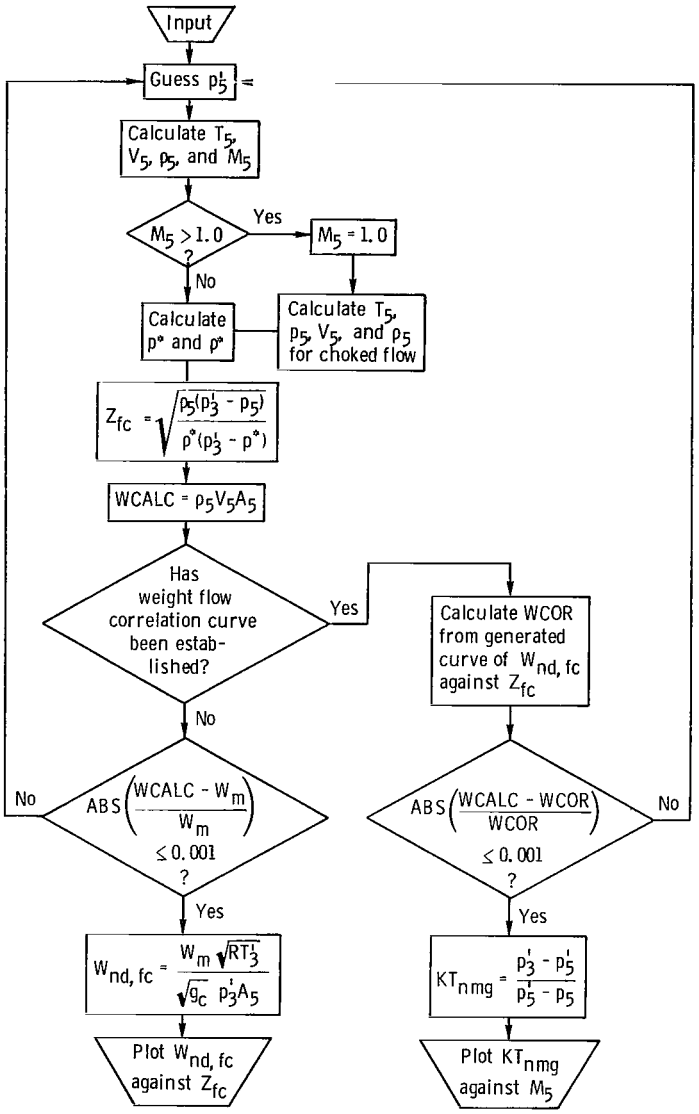

Input:

W_m	measured weight flow
p_3'	total pressure at station 3
T_3'	total temperature at station 3
p_6	static back pressure
A_5	area of film cooling holes
R	gas constant
$\gamma(T)$	ratio of specific heats as function of temperature
$W_{nd, fc}(Z_{fc})$	$W_{nd, fc}$ as function of Z_{fc} (established in first pass through calculations)

Assumptions:

$p_5 = p_6$

$T_5' = T_3'$

Figure 17. - Flow chart for film cooling total-pressure-loss coefficient determination.

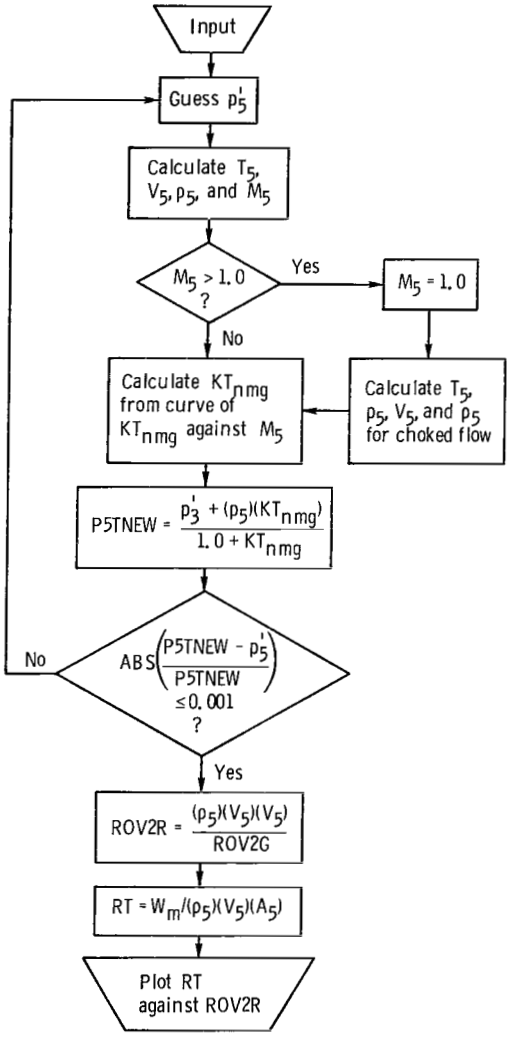

Input:

W_m	measured weight flow
p_3'	total pressure at station 3
T_3'	total temperature at station 3
p_6	static back pressure
A_5	area of film cooling holes
R	gas constant
ROV2G	$(\rho)(V^2)$ of main-stream gas
$\gamma(T)$	ratio of specific heats as function of temperature
$KT_{nmg}(M_5)$	KT_{nmg} as function of M_5

Assumptions:

$p_5 = p_6$

$T_5' = T_3'$

Figure 18. - Flow chart for determination of reduction in film cooling flow due to main-stream gas flow.

REFERENCES

1. Kolodzie, P. A., Jr.; and Van Winkle, M.: Discharge Coefficients Through Perforated Plates. AICHE Journal, vol. 3, no. 3, 1957, pp. 305-312.
2. Damerow, W. P.; et al.: Experimental and Analytical Investigation of the Coolant Flow Characteristics in Cooled Turbine Airfoils. (GE R72AEG165, General Electric Co., NAS3-13499.), NASA CR-120883, 1972.
3. Hippensteele, Steven A.: Pressure-Loss and Flow Coefficients Inside a Chordwise-Finned, Impingement, Convection, and Film Air-Cooled Turbine Vane. NASA TM X-3028, 1974.
4. Rohde, John E.; et al.: Discharge Coefficients for Thick Plate Orifices with Approach Flow Perpendicular and Inclined to the Orifice Axis. NASA TN D-5467, 1969.
5. Smith, M. R.; et al.: Film Cooling Effectiveness from Rows of Holes under Simulated Gas Turbine Conditions. ARC CP-1303, Aeronautical Research Council, 1974. (Supersedes ARC-34738.)
6. Dewey, Paul E.: A Preliminary Investigation of Aerodynamic Characteristics of Small Inclined Air Outlets at Transonic Mach Numbers. NACA TN 3442, 1955.
7. Fluid Meters: Their Theory and Application. Fifth Ed. ASME, 1959.

TABLE I. - TEST GROUPS SUMMARY

Group	Number of runs	Test facility	Plate configuration[a]	Coolant temperature	Main-stream gas temperature	Main-stream gas nominal Mach number
1	21	Tunnel	I and FC	Ambient	Ambient	0
2	4	↓	↓	↓	↓	.2
3	6					.4
4	5					.6
5	5					.8
6	4			↓	↓	.95
7	5			Elevated	Elevated	.6
8	6		↓	Elevated	Elevated	.8
9	5		FC	Ambient	Ambient	0
10	4		↓	↓	↓	.2
11	4					.5
12	4			↓		.9
13	7	↓	↓	Elevated		0
14	23	Bench	I	Ambient		----
15	25	Bench	FC	Ambient	↓	----

[a]I denotes impingement; FC denotes film cooling.

TABLE II. - COMBINED TUNNEL TESTS

Group	Run	Measured weight flow, W_m		Supply total pressure, p_1'		Supply total temperature, T_1'		Plenum total pressure, p_3'		Static back pressure, p_6		Main-stream gas flow total temperature, T_6'		Main-stream gas Mach number, M_g	Parameter $(\rho V^2)_g$	
		kg/sec	lbm/sec	N/cm^2	psia	K	°F	N/cm^2	psia	N/cm^2	psia	K	°F		$kg/(m)(hr^2)$	$lbm/(ft)(hr^2)$
1	358	0.0103	0.0228	12.31	17.86	302	84	10.29	14.93	9.58	13.89	----	----	0	----------	----------
	359	.0147	.0324	14.66	21.26	302	84	10.91	15.83	9.49	13.77	----	----		----------	----------
	360	.0199	.0439	18.10	26.25	303	85	11.92	17.29	9.38	13.61	----	----		----------	----------
	361	.0247	.0545	21.87	31.72	304	87	13.12	19.03	9.29	13.48	----	----		----------	----------
	362	.0308	.0678	26.93	39.06	305	89	15.38	22.30	9.55	13.85	----	----		----------	----------
	374	.0115	.0254	13.18	19.11	296	72	10.73	15.56	9.96	14.44	----	----		----------	----------
	375	.0134	.0296	14.12	20.48	296	72	11.00	15.95	9.96	14.44	----	----		----------	----------
	376	.0173	.0381	16.20	23.49	294	70	11.60	16 82	9.96	14.44	----	----		----------	----------
	377	.0205	.0452	18.71	27.13	294	70	12.33	17.89	9.95	14 43	----	----		----------	----------
	378	.0239	.0527	21.48	31.16	294	69	13.24	19.21			----	----		----------	----------
	379	.0297	.0655	25.86	37.51	293	68	14.84	21.52			----	----		----------	----------
	380	.0363	.0801	31.58	45.80	293	67	17.24	25.00			----	----		----------	----------
	381	.0430	.0949	36.45	52.86	293	67	19.35	28.07			----	----		----------	----------
	382	.0497	.1095	41.87	60.73	292	66	22.01	31.92			----	----		----------	----------
	383	.0149	.0329	14.84	21.52	293	67	11.14	16.15	9.92	14.39	----	----		----------	----------
	384	.0134	.0295	13.89	20.14			10.89	15.79			----	----		----------	----------
	385	.0118	.0260	12.98	18.82			10.64	15.43			----	----		----------	----------
	386	.0095	.0209	12.09	17.53			10.40	15.09			----	----		----------	----------
	387	.0075	.0165	11.41	16.55			10.22	14.82			----	----		----------	----------
	388	.0065	.0143	10.96	15.90			10.11	14.67			----	----		----------	----------
	389	.0051	.0113	10.71	15.53			10.02	14.54			----	----		----------	----------
2	330	0.0199	0.0438	39.38	57.11	299	78	36.64	53.14	35.80	51.92	304	88	0.215	3.025×10^{11}	2.033×10^{11}
	331	.0256	.0565	40.93	59.36	299	79	37.18	53.93	35.88	52.04	303	86	.214	3.017	2.027
	332	.0338	.0746	44.20	64.10	299	79	38.24	55.46	36.08	52.33	304	87	.213	3.025	2.033
	333	.0439	.0968	48.92	70.95	300	80	39.56	57.40	36.11	52.37	304	88	.213	3.025	2.003
3	335	0.0121	0.0267	30.73	44.57	298	76	29.74	43.13	29.17	42.31	303	86	0.397	8.359×10^{11}	5.617×10^{11}
	336	.0218	.0481	33.33	48.34			30.40	44.09	29.08	42.17	302	84	.397	8.294	5.573
	337	.0322	.0710	37.89	54.95			31.73	46.02	29.19	42.34	303	86	.397	8.337	5.602
	338	.0433	.0954	43.95	63.75			33.62	48.76	29.36	42.59	304	87	.395	8.338	5.603
	339	.0542	.1195	50.96	73.91		77	35.71	51.79	29.28	42.46	304	88	.394	8.271	5.558
	340	.0648	.1428	58.86	85.37	299	79	38.44	55.75	29.45	42.71	303	86	.393	8.198	5.509
4	342	0.0130	0.0286	25.02	36.29	299	79	23.48	34.06	22.63	32.82	306	90	0.607	15.145×10^{11}	10.177×10^{11}
	343	.0264	.0583	30.26	43.89	299	79	25.07	36.36	22.65	32.85	304	88	.609	15.221	10.228
	344	.0401	.0884	38.47	55.80	301	81	27.68	40.15	22.81	33.08	306	90	.609	15.291	10.275
	345	.0528	.1165	47.52	68.92	301	82	30.71	44.54	22.81	33.08	307	92	.604	15.117	10.158
	346	.0653	.1440	57.89	83.96	302	84	34.67	50.29	23.10	33.50	306	90	.602	15.066	10.124
5	348	0.0116	0.0255	25.86	37.50	302	83	24.68	35.79	23.78	34.49	307	93	0.804	27.555×10^{11}	18.516×10^{11}
	349	.0178	.0392	27.73	40.22	302	83	25.23	36.59	23.70	34.38	308	94	.804	27.544	18.509
	350	.0376	.0828	37.87	54.93	303	85	28.61	41.50	24.04	34.86	308	95	.802	27.532	18.501
	351	.0557	.1227	50.52	73.27	304	88	32.81	47.59	24.00	34.81	308	95	.805	27.643	18.575
	352	.0653	.1439	58.65	85.07	306	90	35.78	51.90	24.17	35.06	308	94	.798	27.418	18.424
6	353	0.0103	0.0228	23.39	33.93	304	87	22.30	32.35	21.39	31.03	308	94	0.944	33.738×10^{11}	22.671×10^{11}
	354	.0184	.0406	26.30	38.15	304	88	23.52	34.11	21.57	31.28	309	96	.946	33.871	22.760
	355	.0401	.0884	38.53	55.89	305	89	27.45	39.82	21.68	31.45	308	94	.944	33.854	22.749
	356	.0613	.1352	55.07	79.87	306	91	33.30	48.30	21.81	31.63	309	96	.943	33.914	22.789
7	262	0.0139	0.0307	54.16	78.55	762	912	52.15	75.64	51.04	74.03	1146	1603	0.599	30.796×10^{11}	20.694×10^{11}
	261	.0201	.0444	57.07	82.77	776	937	53.12	77.05	51.06	74.05	1146	1603	.599	30.902	20.765
	260	.0259	.0571	59.71	86.60	783	949	53.81	78.05	50.84	73.74	1145	1601	.604	31.242	20.994
	259	.0325	.0716	64.04	92.89	786	955	55.15	79.99	50.85	73.75	1148	1606	.604	31.308	21.038
	258	.0382	.0842	68.44	99.27	787	956	56.23	81.56	50.81	73.70	1146	1602	.608	31.542	21.195
8	267	0.0155	0.0342	43.08	62.48	762	912	40.01	58.03	37.69	54.66	1143	1598	0.816	42.311×10^{11}	28.432×10^{11}
	273	.0176	.0389	44.66	64.77	711	819	40.95	59.40	38.81	56.29	1148	1607	.793	40.819	27.429
	272	.0211	.0466	46.75	67.80	718	832	41.51	60.21	38.63	56.03	1149	1609	.797	41.052	27.586
	274	.0327	.0721	54.69	79.32	706	811	44.30	64.25	38.59	55.97	1149	1609	.792	40.770	27.396
	271	.0325	.0716	54.43	78.94	731	855	43.97	63.77	38.49	55.82	1148	1607	.797	41.055	27.588
	275	.0388	.0856	60.15	87.24	731	856	46.02	66.75	38.65	56.05	1150	1610	.791	40.741	27.377

TABLE III. - SEPARATED TUNNEL TESTS

Group	Run	Measured weight flow, W_m		Plenum total pressure, p_3'		Plenum total temperature, T_3'		Static back pressure, p_6		Main-stream gas flow total temperature, T_6'		Main-stream gas Mach number, M_g	Parameter $(\rho V^2)_g$	
		kg/sec	lbm/sec	N/cm^2	psia	K	^oF	N/cm^2	psia	K	^oF		$kg/(m)(hr^2)$	$lbm/(ft)(hr^2)$
9	433	0.0056	0.0124	9.97	14.46	288	59	9.83	14.25	---	--	0	----------	----------
	434	.0114	.0252	10.52	15.26	289	61	↓	14.25	---	--	↓	----------	----------
	435	.0194	.0427	11.89	17.25	291	64	↓	14.26	---	--	↓	----------	----------
	436	.0251	.0554	13.25	19.22	296	72	↓	14.25	---	--	↓	----------	----------
	437	.0301	.0663	14.64	21.23	294	70	9.77	14.17	---	--	↓	----------	----------
10	439	0.0074	0.0164	30.59	44.37	290	62	30.44	44.15	286	54	0.205	2.323×10^{11}	1.561×10^{11}
	440	.0174	.0383	30.39	44.07	290	62	29.76	43.16	286	54	.207	2.307	1.550
	446	.0327	.0720	32.28	46.82	285	53	30.25	43.88	284	51	.204	2.275	1.529
	443	.0504	.1112	34.97	50.72	288	59	30.12	43.69	285	53	.203	2.261	1.519
11	447	0.00086	0.0019	26.34	38.21	283	49	26.23	38.04	283	50	0.488	11.315×10^{11}	7.603×10^{11}
	448	.0123	.0271	26.92	39.04	277	39	26.27	38.10	284	51	.489	11.377	7.645
	449	.0274	.0604	28.31	41.06	278	41	26.34	38.20	284	52	.488	11.378	7.646
	450	.0456	.1005	31.21	45.26	281	45	26.54	38.49	284	52	.484	11.253	7.562
12	454	0.0034	0.0075	20.01	29.02	284	51	19.57	28.39	287	56	0.847	25.455×10^{11}	17.105×10^{11}
	455	.0176	.0387	20.42	29.62	↓	52	18.71	27.14	↓	56	.860	25.090	16.860
	456	.0352	.0775	23.21	33.67	↓	51	18.82	27.29	↓	57	.859	25.169	16.913
	457	.0515	.1135	27.14	39.37	↓	51	18.87	27.37	↓	57	.856	25.079	16.852
13	473	0.0037	0.0082	10.04	14.56	564	555	9.89	14.35	---	--	0	----------	----------
	472	.0075	.0166	10.56	15.32	604	628	9.87	14.32	---	--	↓	----------	----------
	471	.0133	.0294	11.90	17.26	632	677	9.83	14.25	---	--	↓	----------	----------
	470	.0172	.0380	13.22	19.17	642	696	9.80	14.21	---	--	↓	----------	----------
	469	.0204	.0450	14.55	21.11	652	714	9.80	14.22	---	--	↓	----------	----------
	468	.0271	.0598	18.72	27.15	723	841	9.80	14.21	---	--	↓	----------	----------
	467	.0319	.0703	22.04	31.97	732	857	9.73	14.11	---	--	↓	----------	----------

TABLE IV. - SEPARATED IMPINGEMENT AND FILM COOLING BENCH TESTS

(a) Impingement plate; group 14

Measured weight flow, W_m		Supply total pressure, p_1'		Supply total temperature, T_1'		Static back pressure, p_3	
kg/sec	lbm/sec	N/cm^2	psia	K	^oF	N/cm^2	psia
0.0037	0.0081	10.22	14.83	299	78	9.98	14.47
.0047	.0103	10.36	15.02	298	77		
.0059	.0131	10.59	15.36	298	76		
.0076	.0167	10.96	15.89	297	75		
.0076	.0167	10.96	15.89	296	73		
.0099	.0218	11.59	16.81	↓	↓	↓	↓
.0113	.0249	12.08	17.52				
.0134	.0295	12.96	18.80				
.0158	.0349	14.11	20.47				
.0184	.0406	15.62	22.66				
.0202	.0445	16.79	24.35	297	75		
.0235	.0518	19.31	28.00	298	77	9.97	14.46
.0244	.0539	20.11	29.17	299	78	9.97	14.46
.0243	.0536	20.11	29.17	297	74	9.98	14.47
.0243	.0535	20.11	29.17	298	76	↓	↓
.0265	.0584	21.87	31.72	299	78		
.0292	.0644	24.33	35.29	299	78		
.0320	.0705	26.41	38.30	299	79		
.0357	.0788	29.72	43.10	300	80		
.0223	.0491	18.57	26.93	298	77	10.01	14.52
.0215	.0474	17.94	26.02	299	78	↓	↓
.0206	.0455	17.29	25.08	299	78		
.0228	.0502	18.95	27.49	301	81		

(b) Film cooling plate; group 15

Measured weight flow, W_m		Supply total pressure, p_3'		Supply total temperature, T_3'		Static back pressure, p_6	
kg/sec	lbm/sec	N/cm^2	psia	K	^oF	N/cm^2	psia
0.0099	0.0218	10.45	15.15	299	78	9.87	14.32
.0103	.0227	10.49	15.22	↓	↓	↓	↓
.0177	.0391	11.76	17.06				
.0272	.0600	14.11	20.46				
.0157	.0346	11.33	16.43				
.0271	.0598	14.00	20.30		79		
.0519	.1145	23.35	33.87	300	80		
.0038	.0084	9.98	14.47	301	81	9.89	14.34
.0048	.0106	10.03	14.55	301	81	↓	↓
.0064	.0140	10.14	14.70	300	80		
.0082	.0180	10.29	14.92	↓	↓		
.0104	.0229	10.51	15.24				
.0125	.0275	10.81	15.68				
.0149	.0328	11.20	16.25				
.0210	.0464	12.48	18.10				
.0243	.0535	13.26	19.23				
.0263	.0580	13.87	20.12	301	81		
.0300	.0661	14.99	21.74	301	82		
.0338	.0745	16.31	23.65	302	83		
.0367	.0809	17.36	25.18	302	84		
.0403	.0889	18.75	27.19	303	85		
.0435	.0960	19.97	28.97	303	86		
.0473	.1043	21.58	31.30	303	86		
.0549	.1211	24.67	35.78	304	87		
.0575	.1268	25.87	37.52	304	88		

1. Report No.	2. Government Accession No.	3. Recipient's Catalog No.
NASA TP-1036		

4. Title and Subtitle	5. Report Date
EXPERIMENTAL FLOW COEFFICIENTS OF A FULL-COVERAGE FILM-COOLED-VANE CHAMBER	September 1977
	6. Performing Organization Code
7. Author(s)	8. Performing Organization Report No.
Peter L. Meitner and Steven A. Hippensteele	E-9146
	10. Work Unit No.
9. Performing Organization Name and Address	505-04
NASA Lewis Research Center and U.S. Army Air Mobility R&D Laboratory Cleveland, Ohio 44135	11. Contract or Grant No.
	13. Type of Report and Period Covered
12. Sponsoring Agency Name and Address	Technical Paper
National Aeronautics and Space Administration Washington, D.C. 20546	14. Sponsoring Agency Code

15. Supplementary Notes

16. Abstract

Ambient- and elevated-temperature flow tests were performed on a four-times-actual-size model of an impingement- and film-cooled segment of a core engine turbine vane. Tests were conducted with the impingement and film cooling plates combined to form a chamber and also with each of the individual separated plates. For the combined tests, the proximity of the film cooling plate affected the flow of coolant through the impingement plate, but not conversely. Impingement flow is presented in terms of a discharge coefficient, and the film cooling flow discharging into still air with no main-stream gas flow is presented in terms of a total-pressure-loss coefficient. The effects of main-stream gas flow on discharge from the film cooling holes are evaluated as a function of coolant to main-stream gas momentum flux ratio. A smoothing technique is developed that identifies and helps reduce flow measurement data scatter.

17. Key Words (Suggested by Author(s))	18. Distribution Statement
Flow coefficients Discharge coefficient Film cooling	Unclassified - unlimited STAR Category 07

19. Security Classif. (of this report)	20. Security Classif. (of this page)	21. No. of Pages	22. Price*
Unclassified	Unclassified	30	A03

* For sale by the National Technical Information Service, Springfield, Virginia 22161

NASA-Langley, 1977

594 001 C1 U A 770819 S00903DS
DEPT OF THE AIR FORCE
AF WEAPONS LABORATORY
ATTN: TECHNICAL LIBRARY (SUL)
KIRTLAND AFB NM 87117